Insights on Human Adapted Control of Networked Telepresence and Teleaction Systems

Sandra Hirche and Martin Buss

Institute of Automatic Control Engineering, Technische Universität München
D-80290 Munich, Germany
(Tel: +49 89 289 28395; Fax: +49 89 289 28340; E-mail: {S.Hirche, M.Buss}@ieee.org)

Abstract

Multimodal telepresence and teleaction systems enable a human operator to perform in remote environments through a telerobot and a communication network. The focus of this article is on the networked haptic (force feedback) control system with the key challenges of stability and transparency. Transparency is achieved if the human cannot distinguish between direct and teleinteraction. Human perception plays an important role for transparency evaluation. The first part of this article discusses insights how human haptic perception of the remote environment is affected by communication time delay when using the standard passivation control approach with the wave variable (scattering) transformation to achieve stability. The second line of discussion concentrates on network traffic reduction by a novel psychophysically motivated deadband control approach. Human perception is considered in both approaches and experimental validation results are presented.

1 Introduction

In a multimodal telepresence and teleaction system a human operator commands a remote robot (teleoperator) by manipulating the human system interface (HSI) as depicted in Figure 1. Sensors at the telerobot measure environment interaction, which are then communicated and fed back to the human operator using corresponding multimodal human-system interfaces. Application areas of telepresence and teleaction technology reach from telesurgery, -maintenance to tele-training and -entertainment, see e.g. [1]. Haptic (force) feedback in addition to visual and auditory feedback provides the human operator with more complete information and increases the subjective feeling of presence in the remote environment thereby improving the ability to perform complex tasks [2]. Considering video and audio transmission as state-of-the-art multimedia the focus of this article is on the haptic feedback system.

Transparency – in the sense that the technical systems and communication network should not be felt by the human operator, i.e. the operator should feel as if directly being present and active in the remote environment – is one of the key challenges in telepresence and teleaction systems. In [3] the equality of the mechanical impedance displayed to the human operator and the environment impedance defines transparency. In real systems this transparency requirement is difficult to satisfy [4, 5]. However, according to numerous psychophysical studies the human is not able to perceive arbitrarily small differences in haptic properties [6]. The general goal of our research is to incorporate the knowledge of human haptic perception into transparency evaluation and control design in telepresence systems that are operated over a communication network. As a first step, the main contributions of this article are: 1.) a human perception oriented transparency analysis of the communication time delay, and 2.) the introduction of a novel human perception motivated control approach to reduce the network traffic in haptic telepresence systems.

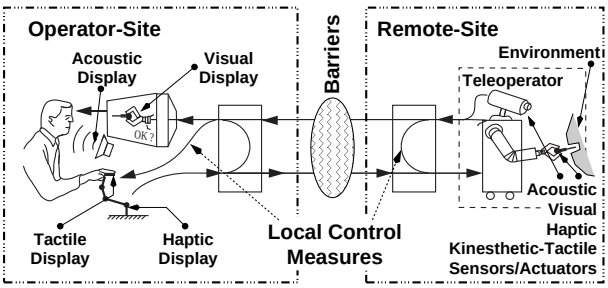

Figure 1: Multimodal telepresence and teleaction system.

In long distance telepresence applications over communication networks such as the Internet, the transmission of the sensor and command data may take up to several hundred milliseconds. By the haptic feedback system a global control loop is closed over the communication network. Due to the communication time delay in the closed loop, the system is unstable without further control measures. A widely used control method guaranteeing stability with arbitrarily large constant time delay is the wave variable transformation [7, 8] (also known as scattering transformation). The extension to the case of time-varying time delay and data loss is very challenging from a control point of view and subject to current re-

search [9–13]. A survey of other control approaches - mostly constrained to constant time delay - can be found in [14].

The first part of this article analyzes how time delay and the wave variable control scheme affect transparency under consideration of human haptic perception. The time delay is assumed constant. The impedance parameters, such as stiffness, damping, and inertia, of the displayed impedance and the environment impedance are compared. A similar analysis for the static case is performed in [15], and in [14] for the comparison of telepresence control schemes; human haptic perception, however, is not considered. In this article, psychophysical results in terms of *just noticeable differences (JND)*, readily available for the impedance parameters [16–18], are used for a human perception oriented interpretation. It is shown that environment mechanical parameters are distorted by communication time delay and the wave variable approach, i.e. a) stiff environments are displayed softer; b) displayable stiffness is upper bounded; c) environment stiffness change perception is reduced; d) in free space motion communication time delay introduces artificial inertia. Transparency in the sense of [3] is not achievable, these requirements can be relaxed, however, using psychophysical insights of JNDs for the mechanical parameters as discussed in this article and validated in experiments.

The second part of the article discusses a communication traffic reduction method for haptic telepresence systems by using a psychophysically motivated deadband control approach. In packet switched communication networks, such as the Internet, data are transmitted in data packets. For stability and performance reasons the haptic command and sensor data are locally continously sampled with rates between 500 and 1000 Hz. It is a common paradigm to transmit every single sample in an individual packet resulting in high data packet rates of 500 to 1000 packets per second to be transmitted over the communication network. High packet rates are, however, hard to maintain over long distance packet switched networks. Further, as the limited communication bandwidth is shared by multiple network applications it is of high interest to reduce the network traffic.

In order to target the problem of communication constraints in the closely related field of networked control systems (NCS) quantization has recently been investigated [19, 20]. Aiming at network traffic reduction in NCS a deadband control approach is proposed in [21]. A data packet is send only if the current value has changed more than a given threshold. This kind of sampling is no longer performed in equidistant time steps and can be considered as event based or Lebesgue sampling, see [22]. Haptic telepresence systems represent a class of NCS, however, due to the largely unknown models of the human and the environment the NCS control approaches cannot directly be carried over. Based on psychophysical insights of human perception a deadband control is proposed with a relative deadband that increases proportionally with the magnitude of the transmitted velocity/force signal corresponding to the JND results for velocity and force signals [6, 23]. The focus in this work is mainly on how human perception characteristics can be used to design transparent haptic telepresence systems. Therefore, in this novel approach to network traffic reduction the communication induced time delay is assumed to be insignificant. As a result the deadband can be directly applied to the velocity/force signals instead of the wave variables. Stability is guaranteed by a passivty based approach. The deadband threshold values are determined in psychophysical experiments where a traffic reduction of about 87% is observed.

The remainder of this article is organized as follows: Section 2 presents the control and psychophysical background; in Section 3 the parameters of the displayed impedance are derived as a function of time delay and the environment impedance by a low frequency approximation. Section 4 gives transparency insights from a human perception point of view, followed by experimental validation in Section 5. The deadband control approach is introduced in Section 6 and validated by experiments in Section 7.

2 Control and Psychophysical Background

The haptic telepresence system basically consists of a force feedback capable HSI (variables indexed $_h$) and the teleoperator (index $_t$) interacting with an usually unknown remote environment (index $_e$) as shown in Figure 2; the blocks of the wave variable transformation are explained in the next section. In bilateral telepresence the human manipulates the HSI applying the force f_h. Based on stability arguments in the standard architecture the HSI velocity $\dot{x}_h$ is communicated to the teleoperator where the local velocity control loop ensures the tracking of the desired teleoperator velocity $\dot{x}_t^d$ (^{d} denotes desired). The force f_e sensed at the remote site, resulting from the interaction with the environment, is transmitted back to the HSI serving as reference signal f_h^d for the lo-

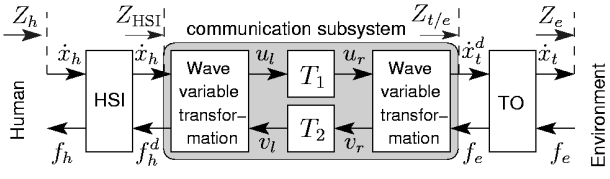

Figure 2: Haptic telepresence system architecture with wave variable transformation.

cal force control. Thereby a global control loop is closed over the communication system. The time delays T_1, T_2 in the forward and backward path, respectively, are assumed to be unknown but constant. Without further control measures the system is unstable due to time delay in the closed loop.

2.1 Stability by Passivity Approach

The passivity concept provides a sufficient condition for stability of the haptic feedback system. A complex system of interconnected network elements (n-ports) is passive if each of the subsystems is passive. A passive element is one for which, given zero energy storage at $t = 0$, the property

$$\int_0^t P_{in}(\tau)\,\mathrm{d}\tau = \int_0^t \boldsymbol{u}^T(\tau)\boldsymbol{y}(\tau)\,\mathrm{d}\tau \geq 0 \quad \forall t > 0 \quad (1)$$

holds, with $P_{in}(\tau)$ denoting the power input to the system, $\boldsymbol{u}(\tau)$, $\boldsymbol{y}(\tau)$ the input and output vector. In classical teleoperation architectures, as proposed in [7], the appropriately locally controlled HSI and teleoperator exchange velocity and force signals. As a result the teleoperator/environment and the human/HSI are considered passive subsystems. The wave variable transformation [7, 8] passifies the communication two-port for arbitrarily large *constant* delays with the transformation equations

$$\begin{aligned} u_l &= \frac{1}{\sqrt{2b}}(f_h^d + b\dot{x}_h)\,; \quad u_r = \frac{1}{\sqrt{2b}}(f_e + b\dot{x}_t^d)\,; \\ v_l &= \frac{1}{\sqrt{2b}}(f_h^d - b\dot{x}_h)\,; \quad v_r = \frac{1}{\sqrt{2b}}(f_e - b\dot{x}_t^d)\ . \end{aligned} \quad (2)$$

The tuning parameter $b > 0$ represents the wave impedance of the communication line.

2.2 Transparency and Human Haptic Perception

The design goal of the haptic feedback system is that the human operator cannot distinguish between direct and teleoperated interaction with an environment. Then the system is called *transparent*. In order to evaluate transparency commonly objective performance metrics are employed. For transparency the position and force at the HSI and the teleoperator are required to be equal in [24]; according to [3] transparency requires the equality of the impedance displayed to the human and the environment impedance

$$Z_h = Z_e, \quad (3)$$

with the mechanical impedance Z defined as the mapping from velocity $\dot{x}$ to force f. In most cases, the considered impedances can be approximated by a linear time invariant system; then the impedance can be represented by the transfer function

$$Z(s) = \frac{f(s)}{\dot{x}(s)}. \quad (4)$$

The transparency requirements are difficult to satisfy in a real system [4, 5], especially with time delay [25]. On the other hand, the human haptic perception characteristics is not incorporated in transparency metrics.

According to numerous psychophysical studies the humans are able to discriminate velocity and force changes which have a magnitude proportional to the signal value itself [6]. The detection threshold, called *just noticable difference* (JND), is empirically determined in psychophysical experiments and represents a statistical quantity. The experimental conditions have a significant influence on the results, this explains the variation for JNDs reported in the literature. The JND for force perception with hand and arm is about 10% [6], for velocity about 8% [23]. Similar detection thresholds exist for the mechanical parameters such as inertia, damping and stiffness. The inertia JND, denoted by JND_m in the following, is about 21% [18](finger); the JND for stiffness perception, denoted by JND_k, is determined to 8% in [17](finger), and 23% in [16](hand/arm).

2.3 Further Assumptions

As the influence of time delay is the major issue in the first part of this article, the dynamics of the teleoperator and the HSI are neglected for this analysis. The teleoperator/environment impedance $Z_{t/e}$, see Figure 2, is considered equal to the environment impedance Z_e, the impedance Z_{HSI} displayed to the HSI equal to the impedance Z_h displayed to the human.

3 Transparency Analysis of Time Delay

The transparency analysis of time delay is performed by the comparison of the impedance parameters displayed to the human and the environment impedance parameters. An analytical approximation of these parameters as a function of time delay is derived in the following. Therefore the displayed impedance Z_h is computed with the reformulated equations (2)

$$Z_h(s) = b\frac{1 + R\,e^{-sT}}{1 - R\,e^{-sT}} \quad \text{with} \quad R = \frac{Z_e - b}{Z_e + b}. \quad (5)$$

and the round-trip time delay $T = T_1 + T_2$. Note that for vanishing delay $T = 0$ the displayed impedance is equal to the environment impedance. The main challenge for an intuitive physical interpretation of the displayed impedance is the complexity of its transfer function (5). Due to the time delay element this transfer function has an infinite number of poles and zeros. Therefore, the displayed impedance is approximated by a lower order system.

3.1 Low Frequency Approximation

The approximation of the displayed impedance transfer function is derived employing the commonly used Padé series of finite order to approximate the delay transfer functions in (5). The order of the displayed impedance approximation depends on the order N of the Padé approximation. A Padé approximation of order N is valid for frequencies $\omega < N/(3T)$. In haptic telepresence systems lower frequencies are of interest as the bandwidth of human haptic (proprioreceptive and kinesthetic) perception is limited to app. 60 Hz. The time delay element is approximated by a first order, i.e. $N = 1$, Padé series

$$e^{-sT} \approx \frac{1 - \frac{T}{2}s}{1 + \frac{T}{2}s}, \tag{6}$$

which is valid for frequencies $\omega < 1/(3T)$. Inserting (6) in (5) yields the approximated displayed impedance

$$Z_h(s) \approx Z_h^{\text{app}}(s) = b\frac{2Z_e + bTs}{2b + TZ_e s} \tag{7}$$

In accordance to the limited frequency range of approximation validity for further analysis this transfer function is split into a low frequency component $Z_{h,lf}^{\text{app}}$ and a high frequency component F_{hf}

$$Z_h^{\text{app}}(s) = Z_{h,lf}^{\text{app}}(s)F_{hf}(s) \tag{8}$$

with the high frequency component having approximately unity gain at lower frequencies

$$|F_{hf}(s)| \approx 1 \quad \text{for} \quad \omega < \frac{1}{3T}. \tag{9}$$

The component $Z_{h,lf}^{\text{app}}$ represents a good approximation of the low frequency behavior of the displayed impedance. The mechanical parameters of the approximated displayed impedance $Z_{h,lf}^{\text{app}}$ can be derived analytically as a function of the round-trip time delay T, the wave impedance b, and the environment impedance Z_e, which is exemplarily carried out in detail for the prototypical cases *free space motion* and *contact with a stiff wall*.

3.2 Prototypical Environment Impedances

3.2.1 Free Space Motion: In free space motion, no environment force is exerted on the teleoperator $f_e = 0$, i.e. the environment impedance is $Z_e = 0$. The exact displayed impedance (5) is

$$Z_h(s) = b\frac{1 - e^{-sT}}{1 + e^{-sT}}.$$

Inserting the environment impedance into (7) gives the approximation of the displayed impedance valid for low frequencies

$$Z_h^{\text{app}}(s) = m_h s\,\frac{1}{\frac{T}{2}s + 1}. \tag{10}$$

with

$$m_h = \frac{bT}{2}. \tag{11}$$

The lefthand factor in (10) represents the low frequency component $Z_{h,lf}^{\text{app}}$ in (8). The righthand factor is the high frequency component F_{hf} satisfying (9); in fact, in steady state $|F_{hf}(0)| = 1$ holds. The similarity of the exact and the approximated displayed impedance for low frequencies can also be observed from their frequency responses for a simulated example, see Figure 3. The displayed impedance is an inertia with the mass m_h (11). A similar result is presented for the static case in [15], its validity is extended here to a low frequencies.

3.2.2 Contact with a Stiff Wall Environment: In contact with a stiff wall, a force proportional to the wall penetration depth with the stiffness k_e acts on the teleoperator; the environment impedance is described by the transfer function $Z_e = k_e/s$. The exact displayed impedance (5) is

$$Z_h(s) = b\frac{k_e + bs + (k_e - bs)e^{-sT}}{k_e + bs - (k_e - bs)e^{-sT}}.$$

The approximation (7) of the displayed impedance for low frequency is analogously computed to the *free space motion* case

$$Z_h^{\text{app}}(s) = \frac{k_h}{s}\left(1 + \frac{bT}{2k_e}s^2\right) \tag{12}$$

with

$$\frac{1}{k_h} = \frac{1}{k_e} + \frac{T}{2b}. \tag{13}$$

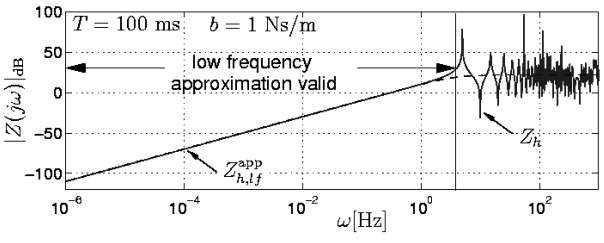

Figure 3: Amplitude/frequency characteristics of the exact and the approximated displayed impedance in *free space motion*.

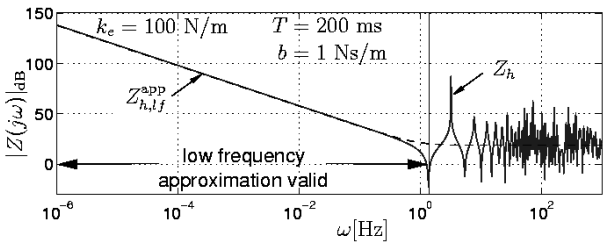

Figure 4: Amplitude/frequency characteristics of the exact and the approximated displayed impedance in *contact with a stiff wall*.

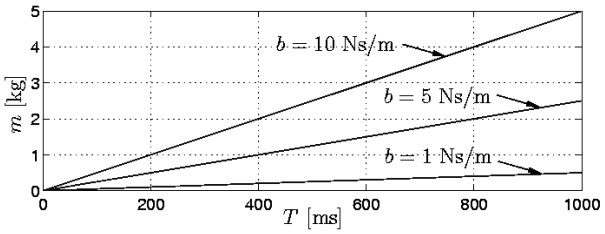

Figure 5: Displayed inertia m_h in *free space motion* depending on round-trip time delay T and wave impedance b.

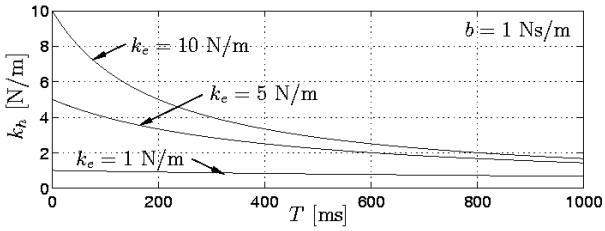

Figure 6: Displayed stiffness k_h in *contact with a stiff wall* depending on round-trip time delay T and environment stiffness k_e.

The lefthand factor $Z_{h,lf}^{\text{app}} = k_h/s$ is the low frequency component from (8). The right hand factor in (12) exhibits high pass behavior satisfying (9); in steady state as in *free space motion* $|F_{hf}(0)| = 1$ holds. A simulation example in Figure 4 shows the frequency responses for the exact and the approximated displayed impedance, which are equal at low frequencies. The displayed impedance in *contact with a stiff wall* has a springlike behavior, however, with a lower stiffness k_h than the environment stiffness k_e. As observable from (13), the communication subsystem including the wave variable transformation can be interpreted as a rod with a stiffness coefficient $2b/T$ in mechanical series connection with the environment.

4 Transparency Insights on Time Delay

The objective and human perception oriented interpretation of the obtained results leads to the following insights.

4.1 Communication Induced Inertia Perception

In *free space motion* an inertia is displayed even though no inertia is contained in the environment. The inertia characteristics is induced by the wave variable transformation and the communication delay. With increasing round-trip time delay T and wave impedance b the displayed inertia m_h proportionally grows (11) as shown in a simulation example in Figure 5. Given a time delay $T > 0$, free space motion is transparent in the sense of (3), i.e. $m_h = 0$, only if $b = 0$ which is unfeasible in terms of the tuning requirement $b > 0$. Considering human perception, an inertia is not perceivable if it is below the absolute human perception threshold Δm for inertia. The empirical value of Δm, though, could not be found in the psychophysical literature. Requiring the displayed inertia to be smaller than this perception threshold $m_h < \Delta m$ results in a relaxed, i.e. feasible, tuning rule $b < 2\Delta m/T$.

4.2 Communication Induced Stiffness Reduction

If the environment exhibits spring characteristics a substantially reduced stiffness is displayed to the human: The environment feels softer than it really is. The displayed stiffness (13) depends on the communication time delay and the environment stiffness as shown in Figure 6. High wave impedance increases the transparency of stiff environments as obvious from (13). In order to achieve transparency in the sense of (3) the wave impedance should be $b \to \infty$, which is unfeasible and contradicts the design requirement for *free space motion*. Considering human haptic perception, for a non-perceivable distortion of the environment stiffness, the displayed stiffness should be reduced by not more than the JND

$$k_h > (1 - \text{JND}_k)k_e,$$

relaxing the transparency requirement (3) according which $k_h = k_e$ should hold. For values of the stiffness detection threshold JND_k refer to Section 2.2. Accordingly, the wave impedance should be tuned to

$$b > \frac{T}{2}(\text{JND}_k^{-1} - 1)k_e,$$

as straightforward derivable from (13). Hence, the consideration of human haptic perception results in a feasible design requirement for transparency.

4.3 Communication Induced Stiffness Bound

The displayed stiffness (13) can never exceed

$$k_{h,\max} = \lim_{k_e \to \infty} k_h = \frac{2b}{T}. \tag{14}$$

This result is also indicated by the asymptotic behavior of the displayed stiffness for increasing environment stiffness shown for a simulation example in Figure 7. Transparency in the sense of (3) is achieved only with $b \to \infty$ (or $T = 0$). However, the human feels a wall to be rigid for a stiffness larger than $k_{\text{rigid}} = 24200$N/m [26]. It is not necessary to display a larger stiffness $k_h \leq k_{\text{rigid}}$ resulting in a relaxed design requirement for the wave impedance b as straightforward derivable from (13).

4.4 Bounded Displayable Stiffness Change

In some tasks not only the absolute value of the displayed stiffness is important but also the possibility to distinguish between differently stiff environments. This

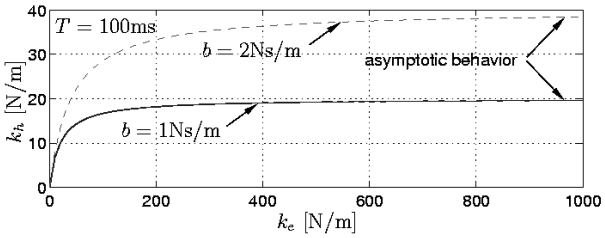

Figure 7: Displayed stiffness k_h depending on environment stiffness k_e and wave impedance b.

is especially important for e.g. tele-surgery applications, where different characteristics have to be distinguished. As indicated by the asymptotic behavior of the displayed stiffness in Figure 7 at higher values of the environment stiffness, a stiffness change in the environment results in a smaller change in the displayed stiffness. However, a change in the environment stiffness from a reference value k_e^0 to the value k_e is perceivable by the human only if the corresponding percentual change in the displayed stiffness

$$\delta k_h = |k_h - k_h^0|/k_h^0 \tag{15}$$

is larger than the stiffness JND

$$\delta k_h = \frac{2b\delta k_e}{2b + Tk_e} \geq \text{JND}_k \tag{16}$$

with the percentual change in the environment stiffness δk_e defined analogously to (15) and the displayed reference stiffness $k_h^0 = k_h(k_e^0)$ according to (13). The percentual change of the displayed stiffness δk_h and the environment stiffness δk_e is equal only for the marginal cases of zero delay $T = 0$ or infinite wave impedance $b \to \infty$. At high delay and high environment stiffness, a large change in the environment stiffness may result in a non-perceivable change of the displayed stiffness. According to (16) a stiffness change is perceivable if the wave impedance is tuned to

$$b \geq \frac{\text{JND}_k T k_e}{2(\delta k_e - \text{JND}_k)},$$

given that the percentual change of the environment stiffness would be perceivable in direct interaction $\delta k_e \geq \text{JND}_k$. The design requirement imposed by (3) is again relaxed by considering human haptic perception characteristics.

4.5 JND for Time Delay

If a delay difference is haptically perceived only by the difference in the mechanical properties of the displayed impedance, a the JND for time delay can be derived from the results from Section 3.2 and the well-known JND's for mechanical properties. This result is interesting with respect to the design of control architectures for telepresence sytems over the Internet, coping with packet loss and time-varying delay, where data buffering strategies, as e.g. in [13], introduce additional delay. If the additional delay is below the human perception threshold then no change in transparency should be perceived.

The percentual difference of the displayed inertia δm_h and the displayed stiffness δk_h, both defined analogously to (15), are considered. The reference values in (15) for the inertia $m_h^0 = m_h(T^0)$ (11) and the stiffness $k_h^0 = k_h(T^0)$ (13) represent the displayed mechanical properties at the reference delay T^0. An absolute time delay difference $\Delta T = |T - T^0|$ is perceivable by the human if the corresponding percentual difference of the displayed mechanical property is larger or equal to the corresponding JND. Accordingly, for *free space motion*

$$\delta m_h \geq \text{JND}_m \tag{17}$$

must hold with JND_m denoting the inertia JND, and for *contact with a stiff wall*

$$\delta k_h \geq \text{JND}_k. \tag{18}$$

Inserting (11) in (17) and (13) in (18) gives the time delay JND for free space motion and contact, respectively. According to that a time delay difference is expected to be perceivable by the human in *free space motion* if

$$\Delta T \geq \text{JND}_m T^0.$$

Due to linear dependence of the displayed inertia in free space motion the time delay JND can be defined as a percentual JND which is equal to the inertia JND. In *contact with a stiff wall* a time delay difference is perceivable by the human if

$$\Delta T \geq \frac{\text{JND}_k}{\text{JND}_k + 1}\Big(\frac{2b}{k_e} + T^0\Big).$$

In contrast to the free space motion case, the JND for time delay depends on the environment stiffness k_e, the wave impedance b and the reference time delay T^0. The detection threshold ΔT becomes smaller with decreasing reference time delay. In both cases, at low reference time delay any additional delay degrades the transparency more than at high reference time delay.

5 Time Delay Experiments

In the first experiment the theoretically obtained dependency of the displayed impedance parameters on the round-trip time delay is validated. In the second one, a preliminary human user study is conducted in order to determine the JND for time delay. In both experiments, the prototypical cases of *free space motion* and *contact with a stiff wall* (stiffness coefficient $k_e = 12500\,\text{N/m}$) are investigated.

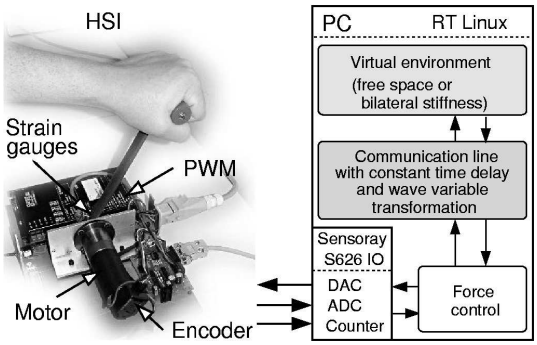

Figure 8: Experimental system architecture.

5.1 Experimental Setup

The experimental setup, see Figure 8, consists of a single degree-of-freedom force feedback paddle, refer to [27] for more details, connected to a PC. The paddle DC motor torque is controlled by the PWM amplifier. The force applied to the paddle lever is measured by a strain gauge bridge, the position of the lever by an optic pulse incremental encoder. A virtual environment is used instead of a real teleoperator/environment in order to seperately consider the prototypical environment scenarios. The virtual environment, the control loops, the model of the communication subsystem with different constant delay and the wave variable transformation with a wave impedance $b = 125\,\mathrm{Ns/m}$ are composed of MATLAB/SIMULINK blocksets; standalone realtime code for RT Linux is automatically generated from that. All experiments were performed with a sample time interval $T_A = 0.001\,\mathrm{s}$.

5.2 Objective Measurements

The displayed inertia m_h in free space motion and the displayed stiffness k_h in contact with the wall are determined depending on the round-trip time delay that is varied within the interval $T \in [5,\ 400]\,\mathrm{ms}$. The parameters m_h and k_h are determined by a least squares identification from the measured HSI position and HSI force signals. The results for the displayed inertia in free space motion are shown in Figure 9 (a) [1], and for the displayed stiffness in contact in Figure 9 (b). The theoretically obtained dependencies of these parameters on the round-trip time delay given by (11) and (13) are convincingly validated. The slightly reduced stiffness and the higher inertia in the experiments result from the limited bandwidth of the conservatively tuned force control loop at the HSI.

5.3 Human User Study

Four experiments with 7 subjects were performed for two different reference round-trip time delays $T^0 = 2\mathrm{ms}$ and $T^0 = 100\mathrm{ms}$ for each of the considered prototypical cases *free space motion* and *contact with a wall* using the same parameters as in the foregoing experiment. The subjects were told to operate with their preferred hand. They were equipped with earphones to mask the sound the device motors generate. The view to the teleoperator device was blocked so no information could be obtained visually.

[1] The inertia results for $T < 100\,\mathrm{ms}$ are missing because of numerical unreliabilities in least squares estimation.

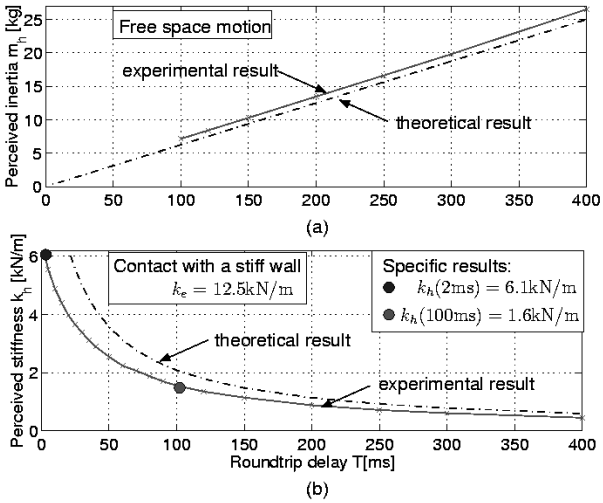

Figure 9: Experimentally obtained displayed inertia m_h (a) and stiffness k_h (b) depending on round-trip time delay T compared to theoretical results.

The well-known three interval forced choice (3IFC) paradigm is used, which is a common experimental tool in psychophysics to determine detection thresholds in human haptic perception [28]. The main feature is that the subjects are presented three consecutive time intervals, 20s each, two with the reference value T^0 of the time delay, one with a different time delay value T. The subject has to tell which of the intervals felt different. Starting from a non-perceivable delay difference ΔT this value is increased after every incorrect answer until three consecutive correct answers on the same value ΔT are given. Three of these passes are performed, the mean value over the passes is considered the subject specific detection threshold.

The results for all four experiments are shown in Figure 10, where $\overline{\Delta T}$ denotes the average over all subjects. As expected from the theoretical results in Section 4.5, in both scenarios, the average detected delay difference is smaller for low reference time delay. Even with this very small number of subjects, for *contact with a stiff wall* the mean detection threshold for low reference delay is statistically significant (95%) smaller than for high reference delay $\overline{\Delta T}_{2\mathrm{ms}} < \overline{\Delta T}_{100\mathrm{ms}}$. For *free space motion* it is not significant (90%) in a statistical sense. For a cross check the percentual changes of the displayed inertia δm_h and stiffness δk_h corresponding to these time delay JNDs

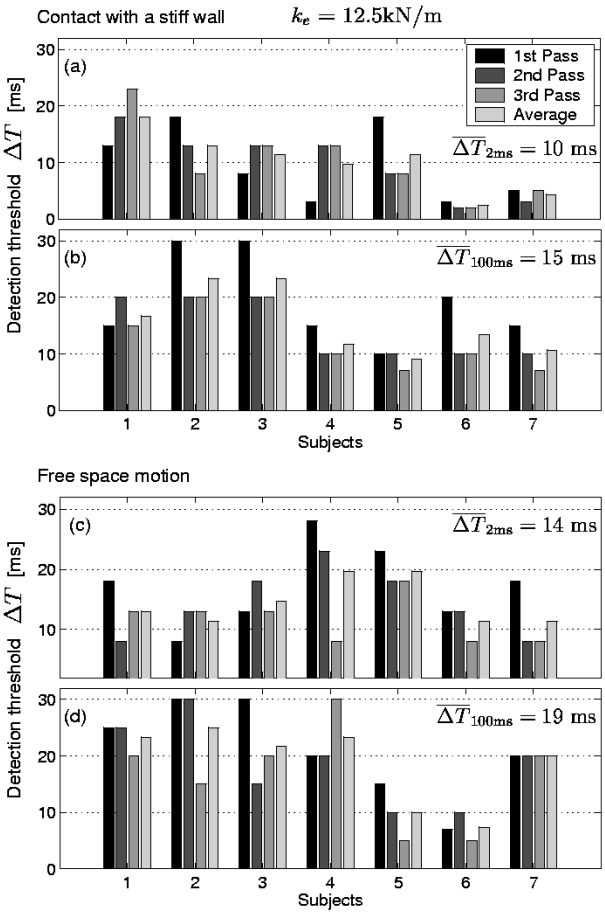

Figure 10: Results of human user study: time delay detection thresholds ΔT for contact with a stiff wall (a), (b) and free space motion (c), (d) at reference time delays $T_0 = 2\,\mathrm{ms}$ (a), (c) and $T_0 = 100\,\mathrm{ms}$ (b), (d).

are computed using the results from the previous experiment. The percentual changes ($\delta m_{h,2\mathrm{ms}} = 17\,\%$, $\delta k_{h,2\mathrm{ms}} = 10\,\%$, $\delta k_{h,100\mathrm{ms}} = 20\,\%$) are, as expected, all in the range of the JNDs reported in literature, see Section 2.2 for comparison. For a reliable statement on the here indicated correspondence of detection thresholds for time delay and mechanical properties a systematic investigation with more subjects is necessary. Further comparative investigations in terms of other human oriented experimental performance indices such as task completion time should evaluate, how a non-perceivable delay difference influences the human task performance.

6 Towards Network Traffic Reduction

In the second part of this article a control strategy to reduce the network traffic in haptic telepresence systems is investigated. The objective is to reduce the network traffic without impairing the perception of the remote environment; i.e. a transparency degradation should not be perceivable. Based on psychophysical insights of human

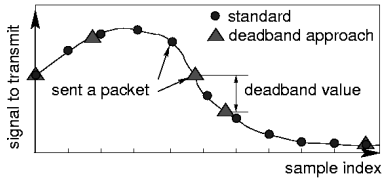

Figure 11: Visualization of the deadband control principle.

perception a deadband control for the transmission of the sampled velocity and force signals is proposed. The focus in this work is mainly on how human perception characteristics can be used to design transparent haptic telepresence systems. Therefore, in this very first approach to network traffic reduction the communication time delay is assumed to be insignificant[2]. As a result the wave variable architecture is not required; the deadband is directly applied to the velocity/force signals instead of the wave variables where no psychophysical results exist.

6.1 Deadband Control

The deadband controller compares the previous value $x(t')$ sent over the network to the most recent value $x(t)$ with $t > t'$; the value x stands here for the transmitted force and velocity signal. If the absolute value of the difference $|x(t) - x(t')|$ is smaller than the deadband width Δ then no update is sent over the network. Otherwise the value $x(t)$ is transmitted and a new deadband is established. The deadband control principle is visualized in Figure 11. The relative deadband grows linearly by factor ϵ with the magnitude of the value $x(t')$. The absolute value Δ of the deadband is then given by

$$\Delta_{x(t')} = \epsilon |x(t')|. \tag{19}$$

As not all data samples are transmitted, deadband control results in empty sampling instances at the receiver side where the transmitted velocity/force signals act as set values to the corresponding control loop. The missing data need to be reconstructed by some reconstruction algorithm. The data reconstruction has an impact on the system stability as shown in [29,30] and briefly discussed in the following.

6.2 Data Reconstruction and Stability

In order to guarantee the stability of the teleoperation system the bilateral communication subsystem should be passive, i.e. the energy balance according to (1) should be non-negative. The communication subsystem includes the deadband algorithm, the communication channel, and the data reconstruction strategy in the forward and the backward path as illustrated in Figure 12. During the time intervals of packet transmission the communication subsystem is passive (lossless). For passivity of the com-

[2] Current investigations are being performed for the time delay case; results will be presented in a forthcoming paper.

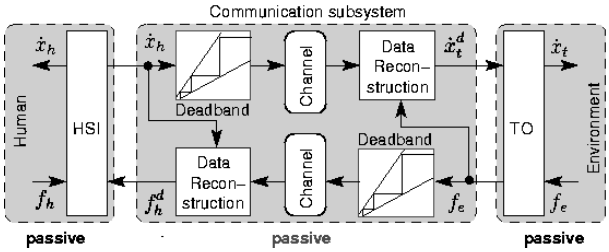

Figure 12: Deadband controlled telepresence system.

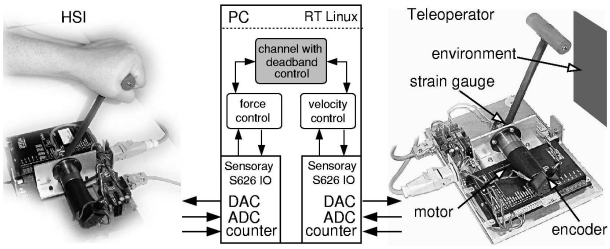

Figure 13: Experimental setup for deadband human user study.

munication subsystem it is sufficient to show, that the energy balance for the time intervals of data reconstruction is non-negative, see [30] for a more detailed discussion. It can be shown that the common reconstruction algorithm "hold last sample" (HLS)

$$\begin{aligned} f_h^d(t) &= f_e(t') \\ \dot{x}_t^d(t) &= \dot{x}_h(t'), \end{aligned}$$

with $\dot{x}_h(t')$ and $f_e(t')$ the values of the most recent packet sent, potentially generates energy. Stability is not guaranteed. The modified HLS proposed in [29]

$$\begin{aligned} f_h^d(t) &= f_e(t') + \Delta_{f_e(t')}\text{sign}\{\dot{x}_h(t)\} \\ \dot{x}_t^d(t) &= \dot{x}_h(t') - \Delta_{\dot{x}_h(t')}\text{sign}\{f_e(t)\}, \end{aligned} \tag{20}$$

with sign denoting the sign function, passifies the communication subsystem and thereby guarantees stability of the telepresences system.

6.3 Position Update

The data reconstruction (20) of the velocity signal induces a velocity error between the HSI and the teleoperator. As a result the teleoperator position may drift from the HSI position. The position drift does not only deteriorate the transparency, but may also drive the system to inoperability if the HSI or the teleoperator reaches the limit of its workspace. In [31] the velocity/force architecture is extended by a position feedforward. It is designed with a saturated position controller at the teleoperator such that the passivity condition is not violated. With the same arguments we propose to send a HSI position update together with the velocity data packets in order to improve the position tracking.

7 Deadband Experiments

Main goal of the human user study is to determine the relative deadband ϵ (19) such that the network traffic is minimized without transparency degradation. Hence the largest non-perceivable deadband, the deadband detection threshold, is of interest and determined in the following preliminary human user study.

7.1 Experimental Setup

The experimental setup consists of two identical 1-DOF haptic displays, see Section 5.1, connected to a PC and a stiff wall as the environment, see Figure 13. In this study the deadband of the force and velocity signal is considered equal. The data reconstruction is performed using thethe modified HLS algorithm (20).

7.2 Human User Study

Altogether 14 subjects (aged 20–50, 3 female, 11 male) were tested for their detection threshold of the deadband parameter ϵ. As in the previous human user study for time delay the 3IFC paradigm is used. The subjects were presented with three consecutive 20s intervals in which they should operate the system. In two of the intervals the system worked without the deadband algorithm. In one of the three intervals, which was randomly determined, the deadband algorithm with a certain value ϵ was applied. Every three intervals the subject had to tell which of the intervals felt different than the other two. The experiment started with a deadband parameter $\epsilon = 2.5\%$ and was increased after every incorrect answer up to maximal 25%. When an answer was correct, the same value was used again until 3 consecutive right answers were given. After this first pass, the subjects were told how the distortion feels like and with what kind of technique they should be able to perceive it best. Then the value ϵ was decreased to 2.5% again and successively increased again using the same procedure as before. After another 3 consecutive right answers ϵ was reduced by 50% without telling the subjects and the procedure was repeated. The mean value of ϵ of the three passes was taken as the deadband detection threshold for the specific subject.

The specific results for every subject presented in Figure 14 show that no one managed to feel the distortion introduced by the 2.5% and 5% deadband; 75% of the subjects have a perception threshold that is 13% or higher. The results are in the range of the JND values for force and velocity perception of about 10% and 8% , resp., see Section 2.2 for comparison.

The potential of the relative deadband control approach to reduce network traffic can be seen in Figure 15, where the

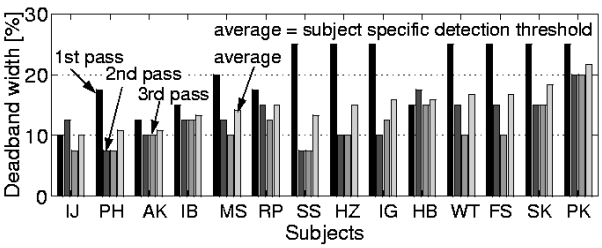

Figure 14: Overview of the subjects' results.

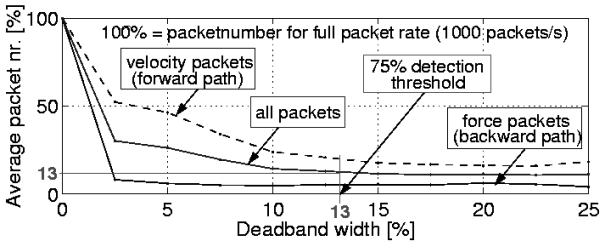

Figure 15: Influence of the deadband on network traffic.

average number of transmitted packets measured during the psychophysical experiments is depicted as a function of the deadband width. The amount of 100% corresponds to the network traffic induced by the standard approach where 1000 packets/s are sent. The network traffic induced by the velocity packets is only 21% of the standard approach at a deadband size of $\epsilon = 13\%$ and further decreases with increasing deadband size. The network traffic characteristics for force packets shows an even better behavior; already at $\epsilon = 2.5\%$ a network traffic reduction by more than 90% is observed. At the 75% deadband detection threshold $\epsilon = 13\%$ a traffic reduction by 87% is observed, i.e. only 13% of the packets containing haptic information need to be transmitted without perceivably impairing transparency.

8 Conclusions

In this article it is demonstrated how human haptic perception can be included into the analysis and design of networked haptic telepresence and teleaction systems. A method for the transparency analysis of haptic (force feedback) telepresence systems is presented with the goal to quantify the degradation induced by communication effects from a human perception point of view. Therefore the effect of communication time delay and the wave variable (scattering) transformation on the mechanical properties of the impedance displayed to the human is analyzed. The interpretation of the results using known psychophysical facts reveals important insights with implications for the control design and the range of teleapplications depending on the communication time delay: a) stiff environments are displayed softer; b) displayable stiffness is upper bounded; c) environment stiffness change perception is reduced; d) in free space motion communication time delay introduces artificial inertia. The prototypical scenarios of the teleoperator in free motion and in contact with stiff environments are investigated theoretically and experimentally, both in objective experiments and human user studies.

In order to reduce the network traffic a human adapted deadband control approach with the deadband chosen in psychophysical experiments is proposed. Stability is guaranteed by a passivity based approach. The communication network traffic is significantly reduced without impairing the perception of the remote environment; in experiments a reduction by 80-90% is observed. Further studies consider traffic reduction in multi-DoF haptic telepresence systems, and the time delay case.

The longterm future goal is to develop a general framework for a human oriented approach to the analysis and design of haptic telepresence and teleaction systems.

Acknowledgments

The psychophysically motivated deadband control strategies have been developed in close collaboration with P. Hinterseer and E. Steinbach. This work is supported in part by the DFG Collaborative Research Center SFB453 and Technische Universität München.

References

[1] M. Buss and G. Schmidt, "Control Problems in Multi-Modal Telepresence Systems," in *Advances in Control: Highlights of the 5th European Control Conference ECC'99 in Karlsruhe, Germany*, P.M. Frank, Ed., pp. 65–101. Springer, 1999.

[2] T.B. Sheridan, *Telerobotics, Automation, and Human Supervisory Control*, MIT Press, Cambridge, Massachusetts, 1992.

[3] D.A. Lawrence, "Stability and Transparency in Bilateral Teleoperation," *IEEE Transactions on Robotics and Automation*, vol. 9, no. 5, pp. 624–637, October 1993.

[4] B. Hannaford, "Stability and Performance Tradeoffs in Bi-Lateral Telemanipulation," in *Proceedings of the IEEE International Conference on Robotics and Automation*, Scottsdale (AZ), US, 1989, pp. 1764–1767.

[5] K. Hashtrudi-Zaad and S.E. Salcudean, "Analysis and Evaluation of Stability and Performance Robustness for Teleoperation Control Architectures," in *Proceedings of the IEEE International Conference on Robotics and Automation*, San Francisco (CA), US, 2000, pp. 3107–3113.

[6] G.C. Burdea, *Force and Touch Feedback for Virtual Reality*, John Wiley, 1996.

[7] R.J. Anderson and M.W. Spong, "Bilateral Control of Teleoperators with Time Delay," *IEEE Transactions on Automatic Control*, vol. 34, no. 5, pp. 494–501, 1989.

[8] G. Niemeyer and J.-J.E. Slotine, "Stable Adaptive Teleoperation," *IEEE Journal of Oceanic Engineering*, vol. 16, no. 1, pp. 152–162, January 1991.

[9] Y. Yokokohji, T. Imaida, and T. Yoshikawa, "Bilateral Control with Energy Balance Monitoring under Time-Varying Communication Delay," in *Proceedings of the IEEE International Conference on Robotics and Automation*, San Francisco (CA), US, 2000, pp. 2684–2689.

[10] R. Lozano, N. Chopra, and M. Spong, "Passivation of Force Reflecting Bilateral Teleoperators with Time Varying Delay," in *Proceedings of the 8. Mechatronics Forum*, Enschede, Netherlands, 2002, pp. 954–962.

[11] S. Munir and W.J. Book, "Control Technique and Programming Issues for Time Delayed Internet Based Teleoperation," *Journal of Dynamic System Measurement and Control-transactions of the ASME*, vol. 125, no. 2, pp. 205–214, 2003.

[12] S. Hirche and M. Buss, "Packet Loss Effects in Passive Telepresence Systems," in *Proceedings of the 43rd IEEE Conference on Decision and Control*, Nassau, Bahamas, 2004, pp. 4010–4015.

[13] B. Berestesky, N. Chopra, and M. W. Spong, "Discrete Time Passivity in Bilateral Teleoperation over the Internet," in *Proceedings of the IEEE International Conference on Robotics and Automation ICRA'04*, New Orleans, US, 2004, pp. 4557–4564.

[14] P. Arcara and C. Melchiorri, "Control Schemes for Teleoperation with Time Delay: A Comparative Study," *Robotics and Autonomous Systems*, vol. 38, no. 1, pp. 49–64, 2002.

[15] G. Niemeyer and J.-J.E. Slotine, "Telemanipulation with Time Delays," *International Journal of Robotic Research*, vol. 23, no. 9, pp. 873–890, September 2004.

[16] L.A. Jones and I.W. Hunter, "A Perceptual Analysis of Stiffness," *Experimental Brain Research*, vol. 79, pp. 150–156, 1990.

[17] Durlach N.I. Beauregard G.L. Tan, H. Z. and M. A. Srinivasan, "Manual Discrimination of Compliance Using Active Pinch Grasp: The Role of Force and Work Cues," *Perception and Psychophysics*, vol. 57, pp. 495–510, 1995.

[18] G.L. Beauregard and M. A. Srinivasan, "The Manual Resolution of Viscosity and Mass," *ASME Dynamic Systems and Control Division*, vol. 1, pp. 657–662, 1995.

[19] W. Wong and R.W. Brocket, "Systems with finite communication bandwidth constraints II: Stabilization with limited information feedback," *IEEE Transactions on Automatic Control*, vol. 44, pp. 1049–1053, 1999.

[20] N. Elia and S.K. Mitter, "Stabilization of linear systems with limited information," *IEEE Transactions on Automatic Control*, vol. 46, pp. 1384–1400, 2001.

[21] P. G. Otanez, J. R. Moyne, and D. M. Tilbury, "Using Deadbands to Reduce Communication in Networked Control Systems," in *Proceedings of the American Control Conference*, Anchorage (AK), US, 2002.

[22] K.J. Aström and B. Bernhardsson, "Comparison of Riemann and Lebesgue Sampling for First Order Stochastic Systems," in *Proceedings of the 41nd IEEE Conference on Decision and Control CDC'02*, Las Vegas (NV), US, 2002, pp. 2011–2016.

[23] L. A. Jones and I. W. Hunter, "Human Operator Perception of Mechanical Variables and Their Effects on Tracking Performance," *ASME Advances in Robotics*, vol. 42, pp. 49–53, 1992.

[24] Y. Yokokohji and T. Yoshikawa, "Bilateral Control of Master-Slave Manipulators for Ideal Kinesthetic Coupling Formulation and Experiment," *IEEE Transactions on Robotics and Automation*, vol. 10, no. 5, pp. 605–619, 1994.

[25] J. Vertut, A. Micaelli, P. Marchal, and J. Guittet, "Short Transmission Delay on a Force Reflective Bilateral Manipulator," in *Proceedings of the 4th Rom-An-Sy*, Zaborow, Poland, 1981, pp. 269–274.

[26] Srinivasan M. A. Eberman B. Tan, H. Z. and B. Cheng, "Human Factors for the Design of Force-Reflecting Haptic Interfaces," *ASME Dynamic Systems and Control Division*, vol. 1, pp. 353–359, 1994.

[27] H. Baier, M. Buss, and G. Schmidt, "Control Mode Switching for Teledrilling Based on a Hybrid System Model," in *Proceedings of the IEEE/ASME International Conference on Advanced Intelligent Mechatronics AIM'97*, Tokyo, Japan, Paper No. 50, 1997.

[28] G.A. Gescheider, *Psychophysics: The Fundamentals*, Lawrence Erlbaum and Associates, 3rd Edition, Hillsdale.

[29] S. Hirche, P. Hinterseer, E. Steinbach, and M. Buss, "Towards Deadband Control in Networked Teleoperation Systems," in *Proceedings IFAC World Congress, International Federation of Automatic Control*, Prague, Czech Republic, 2005.

[30] S. Hirche, *Haptic Telepresence in Packet Switched Communication Networks*, Ph.D. thesis, Technische Universität München, Institute of Automatic Control Engineering, July 2005.

[31] N. Chopra, M.W. Spong, S. Hirche, and M. Buss, "Bilateral Teleoperation over Internet: the Time Varying Delay Problem," in *Proceedings of the American Control Conference*, Denver (CO), US, 2003, pp. 155–160.